ASEAN
Journal of Scientific and Technological Reports
Online ISSN:2773-8752

Research article

Study of Orbit Motion of Hydrogen and Deuterium Beam Ions Toward Neutral Beam Injection Experiment in Thailand Tokamak-1

Pitchayada Wangkhahat[1], Siriyaporn Sangaroon[2*], Apiwat Wisitsorasak[3], Kunihiro Ogawa[4], Nopporn Poolyarat[5], and Mitsutaka Isobe[6]

[1] Faculty of Science, Mahasarakham University, Maha Sarakham, 44150, Thailand; 63010212041@msu.ac.th
[2] Faculty of Science, Mahasarakham University, Maha Sarakham, 44150, Thailand; siriyaporn.s@msu.ac.th
[3] Faculty of Science, King Mongkut's University of Technology Thonburi, Bangkok, 10140, Thailand; apiwat.wis@kmutt.ac.th
[4] National Institute for Fusion Science, National Institutes of Natural Sciences, Toki, 509-5292, Japan and The Graduate University for Advanced Studies, SOKENDAI, Oroshi-cho, Toki, 509-5292, Japan; ogawa.kunihiro@nifs.ac.jp
[5] Thailand Institute of Nuclear Technology, Bangkok, Thailand; nopporn@tint.or.th
[6] National Institute for Fusion Science, National Institutes of Natural Sciences, Toki, 509-5292, Japan and The Graduate University for Advanced Studies, SOKENDAI, Oroshi-cho, Toki, 509-5292, Japan; isobe.mitsutaka@nifs.ac.jp
* Corresponding author: siriyaporn.s@msu.ac.th

Citation:
Wangkhahat, P.; Sangaroon, S.; Wisitsorasak, A.; Ogawa, K.; Poolyarat, N.; Isobe, M. Study of orbit motion of hydrogen and deuterium beam ions toward neutral beam injection experiment in Thailand Tokamak-1. *ASEAN J. Sci. Tech. Report.* **2024**, *27*(1), 58-67. https://doi.org/10.55164/ajstr.v27i1.251121.

Article history:
Received: October 1, 2023
Revised: December 3, 2023
Accepted: December 6, 2023
Available online: December 28, 2023

Abstract: Thailand Tokamak-1 (TT-1) is a small tokamak under the operation of the Thailand Institute of Nuclear Technology. In our future plans, TT-1 has the feasibility of being equipped with external heating systems to achieve high-performance plasma operation and conduct physics associated with fast ions generated by the external heating system. One of the potential external heating systems under consideration is a positive-ion-source-based neutral beam injection (NBI) heating system. The primary source of fast ions for the NBI can be either hydrogen or deuterium-doped hydrogen beams. This study examines how hydrogen and deuterium ions, namely protons and deuterons, respectively, move in orbits, using the Lorentz orbit (LORBIT) code to track their full gyromotion. The energy of the ions has been varied between 200 eV and 40 keV. Three trajectory motions have been characterized, i.e., counter-passing ion, co-passing ion, and trapped ion. The average Larmor radius, dependent on the ion energies, has been investigated. The Larmor radius significantly increases with increasing ion energy in the case of trapped ions, while in the case of counter- and co-passing ions, the Larmor radius exhibits a slight increase with increasing ion energy. Furthermore, the pitch angle range of the lost ion in the TT-1 has been investigated. The results demonstrate the feasibility of utilizing a deuterium-doped hydrogen beam in TT-1 to study fast ion physics. To avoid a large number of lost ions, it is possible to use a deuterium-doped hydrogen beam with an energy not exceeding approximately 10 keV in the TT-1.

Keywords: Thailand Tokamak-1; Neutral Beam Injection; Protons; Deuterons; Lorentz orbit (LORBIT) code

1. Introduction

Fusion energy offers a nearly inexhaustible energy source and very low environmental pollution. To achieve suitable conditions for the fusion reactions on the Earth, plasma must be confined by powerful magnetic fields and

externally heated to multimillion-degree temperatures. One of the most effective external heating is the neutral beam injection (NBI), the primary source of fast ions, including protons and deuterons [1, 2]. Enhancing our understanding of fast ions is one of the important research areas in present-day fusion devices because effective fast ion confinement is essential for achieving high-performance plasmas [3]. In medium-sized fusion devices, such as the Compact Helical System (CHS) with a major radius of 1 m and a minor radius of 0.2 m, a 1% deuterium-doped hydrogen NBI with a beam energy typically ranging from 35 to 40 keV was employed to study fast ion physics [4, 5].

Thailand is well aware of the impact of fusion technology and has a national plan for establishing a fusion research center. With support from the Chinese Academy of Sciences (ASIPP), the Thailand Institute of Nuclear Technology (TINT) is operating Thailand-Tokamak 1 (TT-1), which originated from a former device, HT-6M [6]. The installation of TT-1 at TINT's headquarters in Nakhonnayok province, Thailand, was completed at the beginning of 2023. TT-1 is the small-size tokamak with a major radius of 0.65 m and a minor radius of 0.21 m. It can increase the plasma current (I_p) to 100 kA and the toroidal magnetic field strength (B_t) to 1.52 T. The first plasma was achieved in July 2023. In our plans, TT-1 will be equipped with external heating systems to achieve high-performance plasma operation and conduct physics associated with fast ions generated by external heating systems. One of the planned external heating systems will be a positive-ion-source-based neutral beam injection (NBI) heating system [7, 8]. The first phase will employ an NBI equipped with a hydrogen beam. Deuterium-doped hydrogen beams are considered to enhance high-performance plasma conditions further. The ultimate goal of this work is to conduct a numerical investigation into the behavior of hydrogen and deuterium ions, namely protons and deuterons, respectively, by utilizing the collisionless LORBIT code [9] to track their full gyromotion in TT-1. This analysis will directly support the experimental plan's feasibility for achieving high-performance plasmas in TT-1 using NBI heating utilizing the hydrogen and deuterium-doped hydrogen NBI. This paper is structured as follows: section 2 describes the simulation setup, section 3 presents the results and discussion, and section 4 concludes with a summary.

2. Simulation setup

In this work, the orbit motions of protons and deuterons were tracked using the LORBIT code developed by the National Institute for Fusion Science, Japan [9]. This code has been widely employed for calculating the gyromotion of fast ions in various magnetic confinement systems such as in the LHD [10, 11], EAST [12], KSTAR [13], CFQS [14], Wendelstein 7-X [15], HL-2A and HL-2M [16]. In these works, the deuterons of the NBI source have been tracked to characterize the beam ion motion and study the prompt loss of beam ions for the design of fast ion loss diagnostics [15]. The LORBIT code has also been employed to study the behavior of fusion-born high-energy particles such as tritons and alphas [12]. An overview of the setup used to obtain the orbit motions of protons and deuterons is shown in Figure 1. The calculation in the LORBIT was linked to the magnetic field equilibrium. Here, the magnetic field equilibrium within TT-1 was determined using the FreeGS code, which solves the Grad-Shafranov equation with free boundary conditions [17]. The magnetic field equilibrium was provided for a plasma with ~~an~~ I_p of 100 kA, B_t of 1 T, and magnetic axis position (R_{ax}) of 0.67 m. I_p was clockwise, and B_t was counterclockwise as viewed from the top. It was reported that in the TT-1, the prompt lost beam ion occurs at a time less than approximately 10^{-6} s [7, 8]. Thus, this calculation set the orbit-following time to 10^{-4} s, high enough to track the deposited injected ion. Each ion was launched with the initial position fixed at a cylindrical coordinate of (r_0, ϕ_0, z_0) = (0.72 m, 0, 0) as shown in Figure 2a). The initial velocity along the z-axis (v_z) was assumed to be zero. Additionally, velocity along the x-axis (v_x) and velocity along the y-axis (v_y) were varied for the initial velocity vector ($\boldsymbol{v}$) to allow for the ion's initial pitch angle (χ_0) to range from 0° to 180°. Note that the pitch angle was calculated by determining the angle between the $\boldsymbol{v}$ at the deposition position and the local direction of the $\boldsymbol{B}$, i.e., χ is defined as $\chi = \arccos(v_{\parallel}/v)$, where $v_{\parallel}$ represents the parallel ion velocity concerning the local direction of $\boldsymbol{B}$. In this work, we varied the initial energy of protons and deuterons between 200 eV and 40 keV. In the collisionless motion, the total energy of the ion was constant along the trajectory. Furthermore, we employed the vacuum vessel geometry of TT-1 in the LORBIT calculation to study ion confinement and loss properties. Ions were considered lost when crossing with the last close flux surface (LCFS) and colliding with the vacuum vessel. Ion motion is determined by

solving the equation of motion subjected to the Lorentz force, i.e., $m\mathrm{d}\boldsymbol{v}/dt = q(\boldsymbol{v}\times\boldsymbol{B}+\boldsymbol{E})$, where m is the mass of the proton (m = 1.67377 × 10^{-27} kg) or deuteron (m = 3.34359 × 10^{-27} kg), $\boldsymbol{v}$ is its relative velocity, q is the charge of the proton (q = 1.60219 × 10^{-19} C) or deuteron (q = 1.60219 × 10^{-19} C), $\boldsymbol{B}$ is the magnetic field and $\boldsymbol{E}$ is electric field. Note that $\boldsymbol{E}$ is excluded in the LORBIT calculation because the plasma's potential is usually significantly lower than the beam ions' energy. By tracking the ion's trajectory, we can analyze its motion within the TT-1. To validate the orbit motions of protons and deuterons in the TT-1, we calculated the average Larmor radius along the trajectory of each ion and the guiding center trajectory (see Figure 2b)). Note that the Larmor radius is given by $\rho_L = mv_\perp/ZeB$, where m is the mass of the proton or deuteron, $v_\perp$ is the relative perpendicular velocity, Ze is the charge of the proton (Ze = 1.60219 × 10^{-19} C) or deuteron (Ze = 1.60219 × 10^{-19} C), and B is the magnetic field. The guiding center trajectory was calculated using the MATLAB function called Envelope Extraction [18].

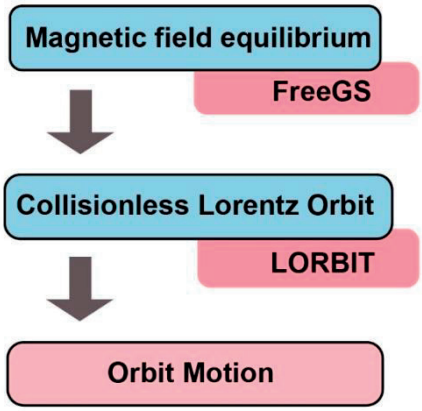

Figure 1. Flowchart to calculate the motion of the hydrogen and deuterium beam ions in orbits using the LORBIT code to track their full gyromotion.

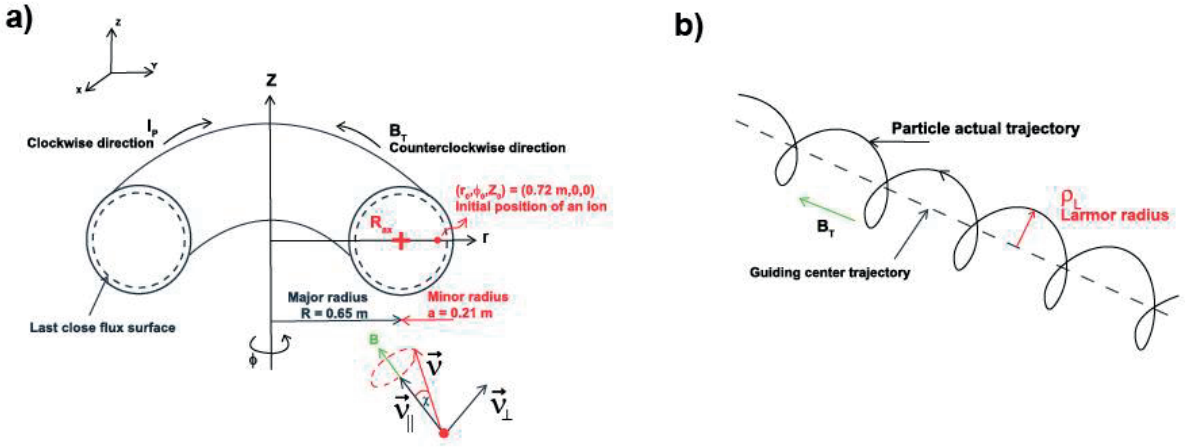

Figure 2. a) The diagram shows the TT-1 torus, vacuum vessel, last close flux surface, initial position of an ion, and its velocity. b) The diagram shows the actual particle and guiding center trajectories where the Larmor radius is defined.

3. Results and Discussion

The results of the averaged Larmor radius along the trajectory and the guiding center trajectory of protons and deuterons in the TT-1 are reported in this section.

3.1 Characterization of ion motion in TT-1

Figure 3a) illustrates the orbit motion of protons, while Figure 3b) depicts the orbit motion of deuterons in a poloidal view. For these calculations, the initial position of the ions was located at (r_0, ϕ_0, z_0) = (0.72 m, 0, 0), and the initial energy of both protons and deuterons was set to 20 keV. In this study, we varied the velocities along the x-axis (v_x) and y-axis (v_y) to allow the ion's initial pitch angle to range from 0° to 180°. We observed that the trajectories of protons and deuterons exhibit four distinct types of motion: counter-passing ion, co-passing ion, trapped ion, and ion loss. The counter-passing ion is classified by shifting inward concerning the magnetic axis of ion motion. In contrast, the co-passing ion is classified by shifting outward concerning the magnetic axis of ion motion. The trapped ion is classified into a banana shape. All trajectories characterized as a counter-passing ion, co-passing ion, and trapped ion remained confined within TT-1 without impacting the vacuum vessel, in other words, without crossing the LCFS, while ion loss occurred when ions crossed the LCFS and hit the vacuum vessel. Enhancing our understanding of fast ion confinement and loss behavior in the TT-1 is one of the important issues for achieving high-performance plasmas in future operations using NBI heating. The motion of ions depends on the pitch angle, and we have summarized the pitch angle range data for protons and deuterons in Table 1. The ion loss ranges for proton and deuteron occurs at angles resulting in the upper region of counter-passing ions, as the ions have high parallel velocity ($v_{||} >> v_{\perp}$) with co-direction with the magnetic field (low pitch angle), and the curvature drift is dominant for the drift orbit. In TT-1, it is found that the lost beam ions move upward due to ion curvature drift, and thus, the lost positions are located on the upper panel of the vacuum vessel (see Figures 3 and 4). It is clear that even though protons and deuterons exhibit the same characteristic motion and pitch angles, their Larmor radius significantly differs due to their mass differences. Deuterons show a wide range of pitch angles, which can result in ion loss. Figure 4a) displays the typical collisionless proton orbits depicting counter-passing ion confinement and ion loss in a three-dimensional view. The lost beam ions are classified into a fat banana orbit and collide with the vacuum vessel. Figure 4b) illustrates the extracted guiding center trajectory of these actual motions in poloidal projection.

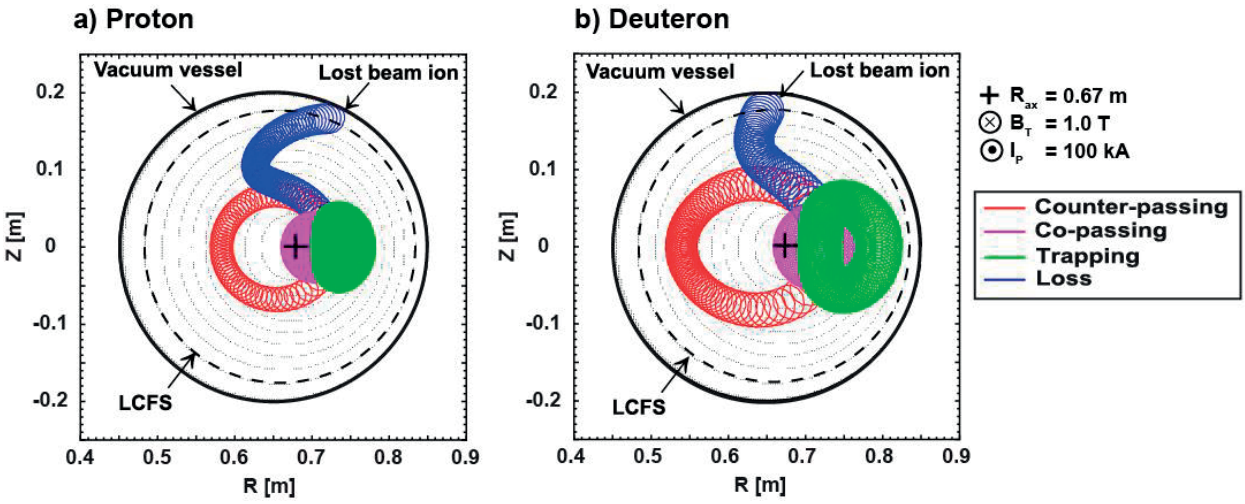

Figure 3. a) Examples of the trajectories of the counter-passing ion (red), co-passing ion (magenta), trapped ion (green), and loss ion (blue) of proton in poloidal view of TT-1 when the initial pitch angles of hydrogen were set to be 50°, 105 °, 89 °, and 66 °, respectively. b) Examples of the trajectories of the counter-passing ion (red), co-passing ion (magenta), trapped ion (green), and loss ion (blue) of the deuteron in the poloidal view of TT-1 when the initial pitch angles of hydrogen were set to be 50°, 105 °, 89 °, and 66 °, respectively. Note that the initial position of the ions was located at (r_0, ϕ_0, z_0) = (0.72 m, 0, 0), and ion energy was 20 keV.

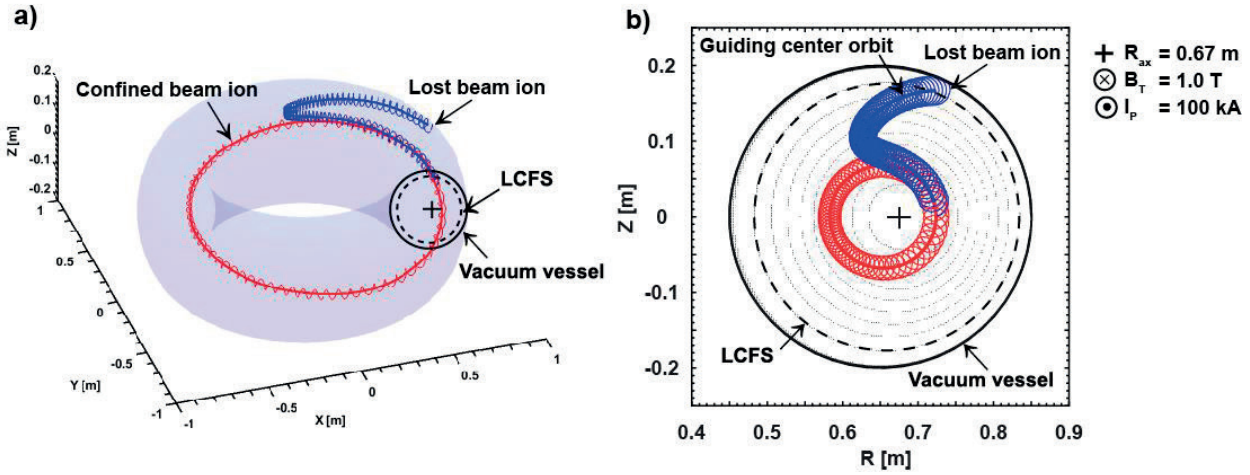

Figure 4. Typical collisionless proton orbits were calculated by the LORBIT code in a) three-dimensional view and b) poloidal projection. The figures show the actual particle and guiding center trajectories (thick lines). Lost beam ions (blue) are classified into a fat banana orbit and hit the vacuum vessel, while confined beam ions (red) exhibit counter-passing ion orbits and are well-confined.

Table 1. Relationship between the motion and pitch angle range of protons and deuterons.

Ion type	Motion type	Range of pitch angle
Proton	counter-passing ion	0˚ - ~ 60˚
	co-passing ion	~ 100˚ - ~ 180˚
	trapped ion	~ 75˚ - ~ 100˚
	loss ion	~ 60˚- ~ 75˚
Deuteron	counter-passing ion	0˚ - ~ 50˚
	co-passing ion	~ 100˚ - ~ 180˚
	trapped ion	~ 85˚ - ~ 100˚
	loss ion	~ 50˚- ~ 85˚

3.2 The impact of energy on confined ion motion

In this study, we varied the energy of protons and deuterons in the range of 200 eV to 40 keV to investigate how energy affects ion confinement motion. Figures 5a) and 5b) depict the trajectories of confined protons when the ion has an energy of 2 keV and 10 keV, respectively. Larmor radius is given by $\rho_\perp = mv_\perp/ZeB$, where $v_\perp$ is proportional to the ion energy. Consequently, as the ion energy increases, the Larmor radius of ions also increases. It is evident in this work that the orbital motion, in other words, Larmor radius, increases with higher energy. Similarly to the proton motion, the confined deuteron trajectories are shown in Figures 5c) and 5d). The results show that the orbital motion of deuterons, in other words, Larmor radius, increases with higher energy. The Larmor radius of protons and deuterons was calculated and is displayed in Figure 6a) for counter-passing ions, Figure 6b) for co-passing ions, and Figure 6c) for trapped ions. In the counter-passing ion case, the Larmor radius slightly increases from 0.04 cm to 0.60 cm for protons and from 0.05 cm to 0.91 cm for deuterons when the ion's energy increases from a few eV to an extremely high energy of 40 keV. It is found that deuterons have almost the same Larmor radius as protons at low energy and are approximately 52 % larger at an extremely high energy of 40 keV. In the co-passing ion case, the Larmor radius slightly increases from 0.04 cm to 0.48 cm for protons and from 0.05 cm to 0.68 cm for deuterons when the ion's energy increases from a few eV to an extremely high energy of 40 keV. It is found that deuterons have almost the same Larmor radius as protons at low energy and are approximately 42 % larger at an extremely high energy of 40 keV. In the trapping case, the Larmor radius significantly increases from 0.21 cm to 3.00 cm for protons

and from 0.30 cm to 4.23 cm for deuterons when the ion's energy increases from a few eV to an extremely high energy of 40 keV. It is found that deuterons' Larmor radius is approximately 42 % larger than a proton's Larmor radius at an ion's energy of 2 keV and approximately 41 % larger than a proton's Larmor radius at an extremely high ion's energy of 40 keV.

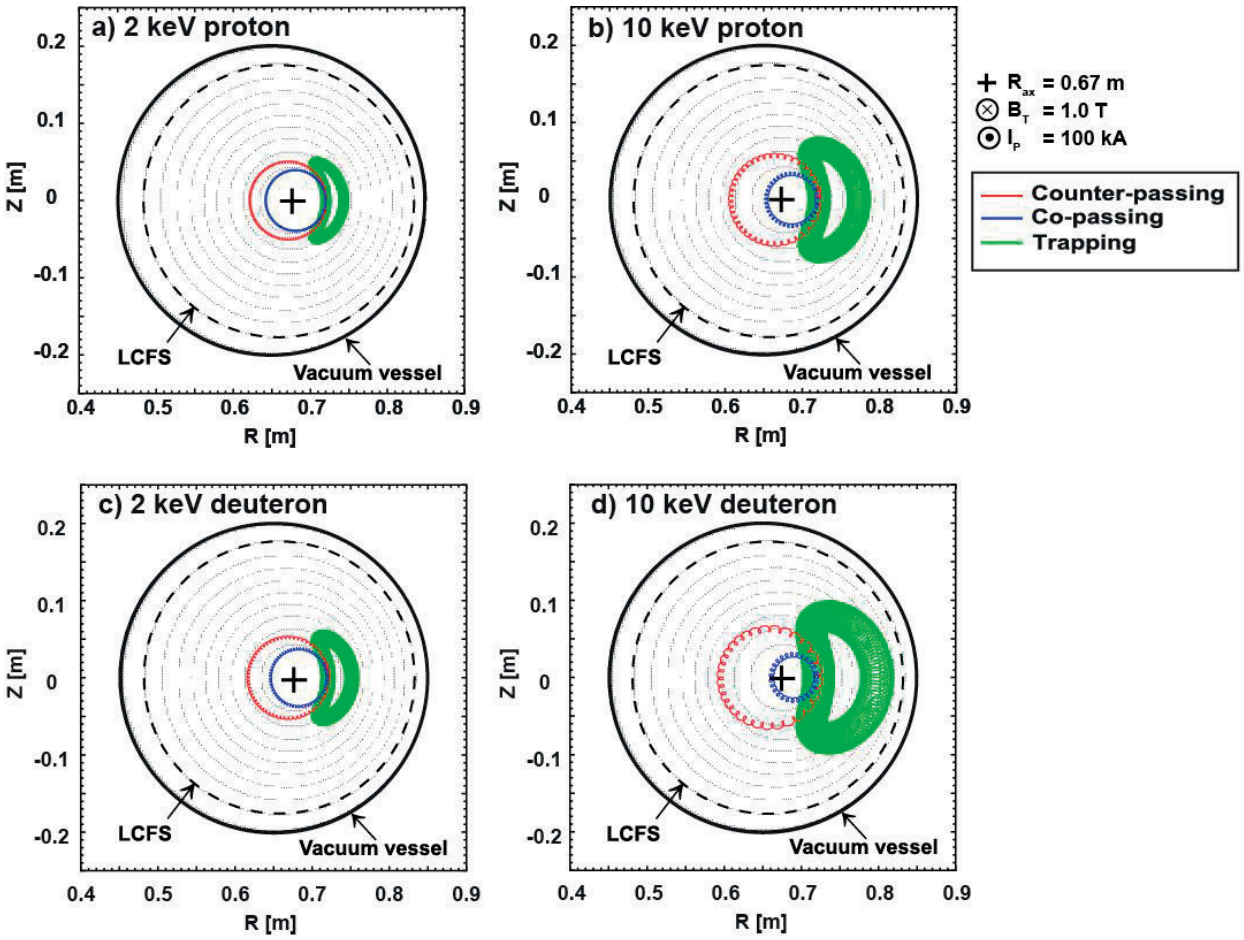

Figure 5. Typical orbit of well-confined ions characterized as counter-passing ion, co-passing ion, and trapped ion of proton with energy of a) 2 keV and b) 10 keV, and deuteron with energy of c) 2 keV and d) 10 keV.

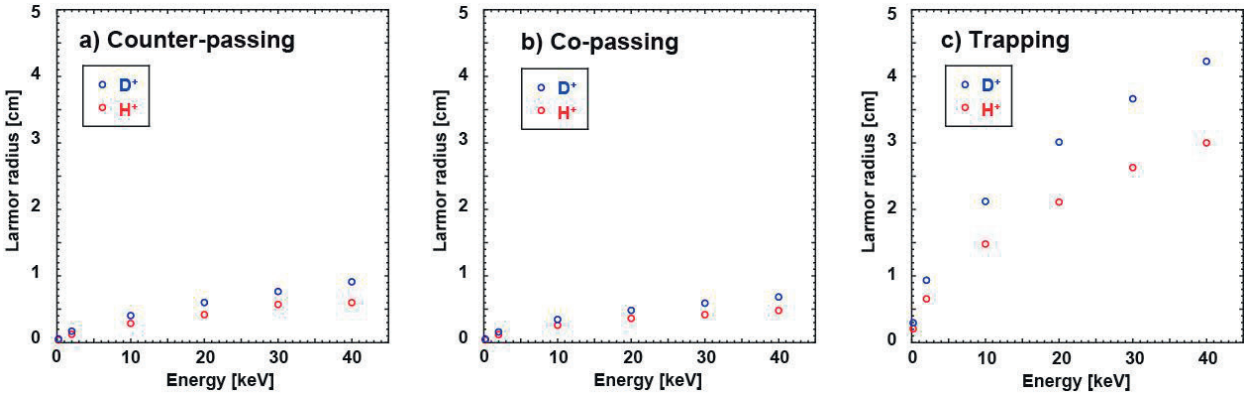

Figure 6. Typical Larmor radius of proton and deuteron characterized by a) counter-passing, b) co-passing, and c) trapping motions.

3.3 The impact of energy on loss ion motion

Most of the lost ions were near the passing and trapped boundary where the trapped ion is classified into a banana shape. The size of the banana orbit can be calculated by considering the motion of a trapped particle in a nonuniform magnetic field. The width of the orbit (W) can be written as $W = 2v_{||}/\omega_{c\theta}$, where $\omega_{c\theta}$ is a gyro-frequency. Since $v_{||}$ is proportional to the ion energy, the size of the banana orbit increases as the ion energy increases. In this evaluation, we assessed the behavior of trapped and lost ions when the pitch angle was fixed at approximately 80° while varying the energy from 200 eV to 40 keV. Figures 7a) and 7b) show the guiding center trajectory of protons and deuterons, respectively. Note that the actual motions were removed for better visibility. As the energy increases, the trajectory width and height of the banana orbit, in other words, the banana shape, become larger. Note that the width of the banana orbit was determined from the maximum trajectory width in the radial direction, and the height of the banana orbit was determined from the maximum trajectory height in the z-axis direction (see Figure 7a)). The protons became lost ions when they had an energy above 20 keV, while the deuterons became lost ions when they had an energy above 10 keV. The width and height of the banana-shaped motion for protons and deuterons, which depended on the ion's energy being lower than the energy that causes the fat banana orbit of a lost ion, were calculated and displayed in Figures 8a) and 8b), respectively. At an ion's energy increased from 200 eV to 10 keV, the results show that the banana shape width significantly increases from 0.01 m to 0.05 m for protons and from 0.01 m to 0.08 m for deuterons. The banana shape width of deuterons was approximately 60 % wider than the banana shape width of protons at an ion's energy of 10 keV. Consequently, the banana shape height significantly increases from 0.08 m to 0.13 m for protons and from 0.08 m to 0.16 m for deuterons. The banana shape height of deuterons was approximately 23 % higher than that of protons.

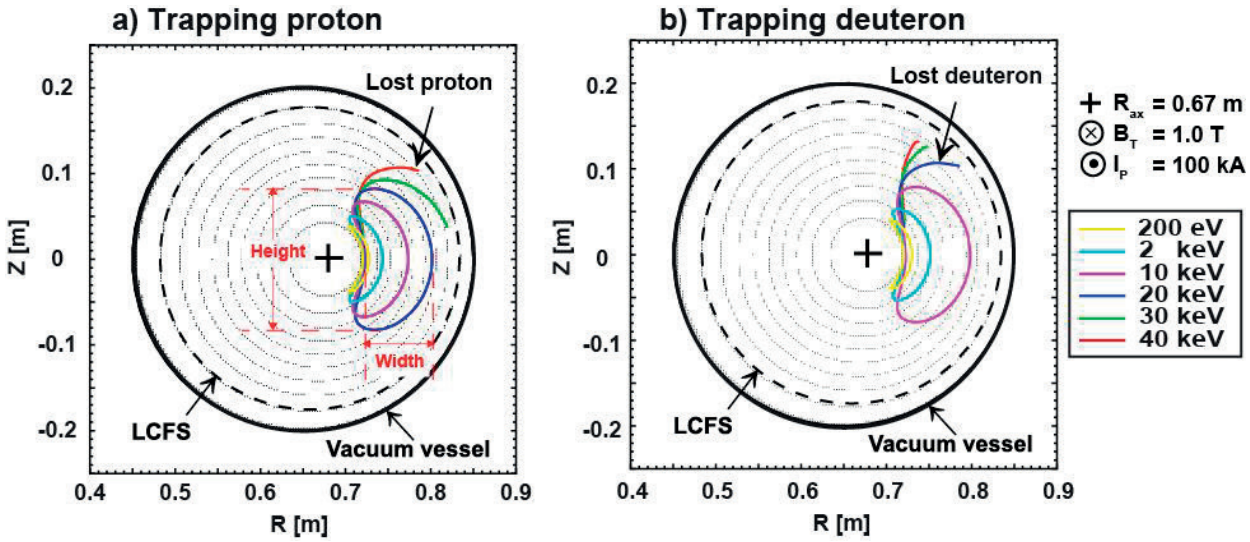

Figure 7. The typical guiding center trajectory of a) protons and b) deuterons was characterized by a banana shape when the pitch angle was fixed at approximately 80° while varying the energy from 200 eV to 40 keV.

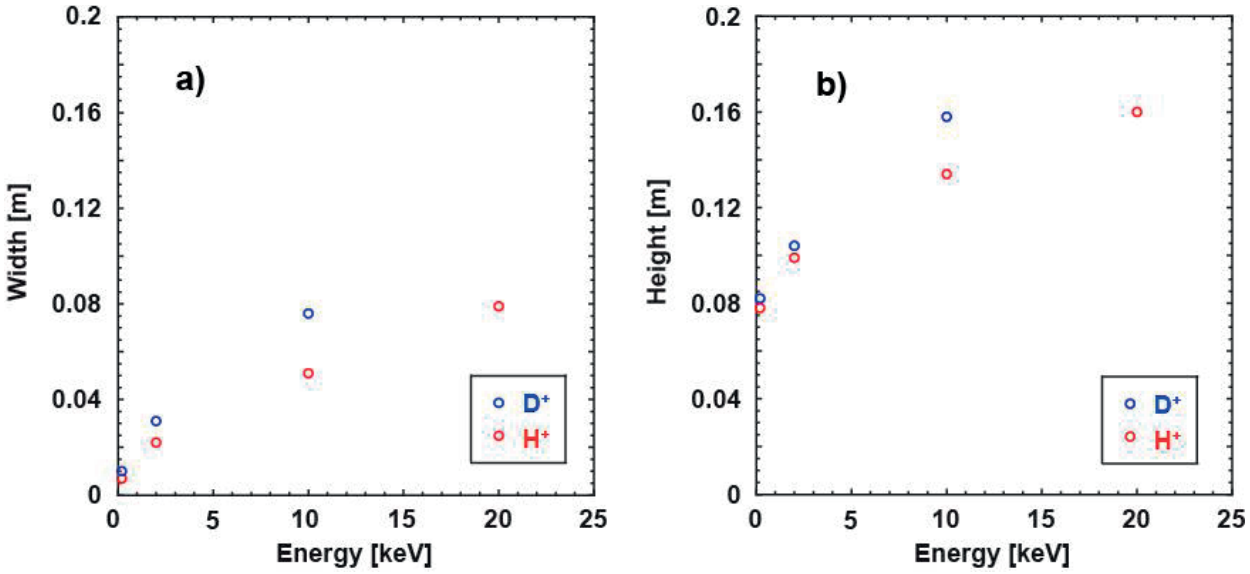

Figure 8. a) The width of the banana orbit, determined from the maximum trajectory width in the radial direction, and b) the height of the banana orbit, determined from the maximum trajectory height in the *z*-axis direction for protons and deuterons versus ion's energy that lower than the energy that causes the fat banana orbit of a lost ion.

4. Conclusions

In our upcoming initiatives, TT-1 is exploring the possibility of integrating external heating systems to enhance plasma performance and investigate the physics associated with fast ions generated by these external heating systems. Among the considered options is a positive-ion-source-based NBI heating system. The NBI plan can utilize hydrogen and deuterium-doped hydrogen beams as its primary ion source. This study focuses on the orbital dynamics of protons and deuterons, employing the collisionless LORBIT code for trajectory tracking. The investigation categorizes three types of confined ion motions: counter-passing ions, co-passing ions, and trapped ions, for both protons and deuterons, which depend on their initial pitch angles. Additionally, we examine how the average Larmor radius, influenced by ion energies, evolves. We observed a significant increase in the Larmor radius with higher ion energy, particularly for trapped ions. In contrast, counter-passing and co-passing ions exhibit a more modest increase in Larmor radius as ion energy rises. The results demonstrate the possibility of using either a hydrogen and/or a deuterium-doped hydrogen NBI in TT-1 to study fast ion physics in plans. In future work, exploring the feasibility and effectiveness of NBI in TT-1 is recommended by utilizing the birth profile of ions computed using the Monte Carlo fast ion module NUBEAM code. The investigation should consider factors such as ion collisions, charge exchange loss and recombination, and the transport of beam ions. The results from this study will directly contribute to shaping the future experimental strategy for achieving high-performance plasmas by utilizing the external heating system, such as the NBI system in TT-1.

5. Acknowledgements

S.S. acknowledged the financial support by the Program Management Unit for Human Resources and Institutional Development, Research and Innovation fiscal year 2023 (Grant No. B37G660016) and by Thailand Science Research and Innovation (TSRI) via Fundamental Fund FY2566 (Contract Number 2589646/4369740). P.W. acknowledged the financial support by the Faculty of Science, Mahasarakham University, in fiscal year 2023 (Grant No. 6601001/2566).

Author Contributions: Conceptualization, S.S., A.W., K.O., M.I.; methodology, P.W.; validation, P.W.; formal analysis, P.W.; investigation, P.W.; data curation, P.W.; writing—original draft preparation, P.W., S.S.;

writing—review and editing, P.W., S.S., A.W., K.O., M.I., N.P; visualization, P.W.; supervision, K.O., M.I.; project administration, N.P.; funding acquisition, S.S., P.W. All authors have read and agreed to the published version of the manuscript.

Funding: Please ensure to include the following statements in your manuscript:

1. "This research was funded by Program Management Unit for Human Resources and Institutional Development, Research and Innovation fiscal year 2023, grant number B37G660016, and by Thailand Science Research and Innovation (TSRI) via Fundamental Fund FY2566, grant number 2589646/4369740, and by Faculty of Science, Mahasarakham University fiscal year 2023, grant number 6601001/2566."
2. "The Article Processing Charges (APC) were funded by the Program Management Unit for Human Resources and Institutional Development, Research, and Innovation for fiscal year 2023, grant number B37G660016."

Conflicts of Interest: The authors declare no conflict of interest. The funders had no role in the design of the study, in the collection, analyses, or interpretation of data, in the writing of the manuscript, or in the decision to publish the results.

References

[1] Sergei Sharapov. *Energetic Particles in Tokamak Plasmas*. CRC Press. **2021.**

[2] Moseev, D.; Salewski, M.; Garcia-Munoz, M.; Geiger, B.; Nocente, M. Recent progress in fast-ion diagnostics for magnetically confined plasmas. *Reviews of Modern Plasma Physics*. **2018**, *2*(7), 1-68. https://doi.org/10.1007/s41614-018-0019-4

[3] Fasoli, A.; Gormenzano, C.; Berk, H. L.; Breizman, B.; Briguglio, S.; Darrow, D. S.; Gorelenkov, N.; Heidbrink, W.W.; Janu, A.; Konovalov, S.V.; Nazikian, R.; Noterdaeme, J.-M.; Sharapov, S.; Shinohara, K.; Testa, D.; Tobita, K.; Todo, Y.; Vlad, G.; Zonca, F. *Chapter 5: Physics of energetic ions*. **2007**, *47*(6), S264-S284. https://doi.org/10.1088/0029-5515/47/6/s05

[4] Isobe, M.; Okamura, S.; Nagaoka, K.; Osakabe, M.; Toi, K.; Yoshimura, Y.; Matsuoka, K.; Sasao, M.; Darrow, D.S. Fast-Ion-Diagnostics for CHS Experiment. *Plasma and Fusion Research*. **2007**, *2*, S1076. https://doi.org/10.1585/pfr.2.s1076

[5] Isobe, M.; Sasao, M.; Okamura, S.; Osakabe, M.; Kubo. S.; Minami, T.; Matsuoka, K.; Takahashi, C.; CHS Group. Experimental Study of Fast Ion Confinement in CHS. *J. Plasma Fusion Res. SERIES*. **1998**, *1*. 366-369.

[6] HT-6M TEAM. Engineering Aspects of The HT-6M Tokamak. *Fusion Technology*. **1986**, *9*(3), 476–480. https://doi.org/10.13182/fst86-a24733

[7] Paenthong, W.; Wisitsorasak, A.; Sangaroon, S.; Promping, J.; Ogawa, K.; Isobe, M. Fast-ion orbit analysis in Thailand Tokamak-1. *Fusion Engineering and Design*. **2022**, *183*, 113254. https://doi.org/10.1016/j.fusengdes.2022.113254

[8] Sangaroon, S.; Ogawa, K.; Isobe, M.; Wisitsorasak, A.; Paenthong, W.; Promping, J.; Poolyarat, N.; Tamman, A.; Ploykrachang, K.; Dangtip, S.; Onjun, T. Feasibility study of neutral beam injection in Thailand Tokamak-1. *Fusion Engineering and Design*. **2023**, *188*, 113419. https://doi.org/10.1016/j.fusengdes.2023.113419

[9] Mitsutaka, I.; Dan, F.; Mamiko, S. Lorentz alpha orbit calculation in search of position suitable for escaping alpha particle diagnostics in ITER. *J. Plasma Fusion Res. SERIES*. **2009**, *43*(4). https://inis.iaea.org/search/search.aspx?orig_q=RN:43003775

[10] Ogawa, K.; Isobe, M.; Nishitani, T.; Murakami, S.; Seki, R.; Nuga, H; Pu, N.; Osakabe, M.; LHD Experiment Group. Study of first orbit losses of 1 MeV tritons using the Lorentz orbit code in the LHD. *Plasma Science & Technology*. **2019**, *21*(2), 025102. https://doi.org/10.1088/2058-6272/aaeba8

[11] Ogawa, K.; Isobe, M.; Nuga, H.; Seki, R.; Ohdachi, S.; Osakabe, M. Evaluation of Alpha Particle Emission Rate Due to the p-^{11}B Fusion Reaction in the Large Helical Device. *Fusion Science and Technology*. **2022**, *78*(3), 175–185. https://doi.org/10.1080/15361055.2021.1973294

[12] Ogawa, K.; Zhong, G.; Zhou, R.; Li, K.; Isobe, M.; Hu, L. 1 MeV Triton Orbit Analysis in EAST Plasmas. *Plasma and Fusion Research*. **2020**, *15*, 2402022. https://doi.org/10.1585/pfr.15.2402022

[13] Jun Young Kim; Rhee, T.; Kim, J.-H.; Yoon, S. W.; Park, B. H.; Isobe, M.; Ogawa, K.; Ko, W. H. Prompt loss of beam ions in KSTAR plasmas. *AIP Advances*. **2016**, *6*, 105013. https://doi.org/10.1063/1.4966588

[14] Ogawa, K.; Isobe, M.; Seki, R.; Nuga, H.; Yamaguchi, H.; Sangaroon, S.; Shimizu, A.; Okamura, S.; Takahashi, H.; Oishi, T.; Kinoshita, S.; Murase, T.; Nakagawa, S.; Tanoue, H.; Osakabe, M.; Liu, H. F.; Xu, Y. Feasibility study of fast ion loss diagnostics for CFQS by beam ion loss calculation on vacuum vessel. *Journal of Instrumentation*. **2021**, *16*(9), C09029. https://doi.org/10.1088/1748-0221/16/09/c09029

[15] Ogawa, K.; Bozhenkov, S. A.; Äkäslompolo, S.; Killer, C.; Grulke, O.; Nicolai, D.; Satheeswaran, G.; Isobe, M.; Osakabe, M.; Yokoyama, M.; Wolf, R. C. Energy-and-pitch-angle-resolved escaping beam ion measurements by Faraday-cup-based fast-ion loss detector in Wendelstein 7-X. *Journal of Instrumentation*. **2019**, *14*(9), C09021. https://doi.org/10.1088/1748-0221/14/09/c09021

[16] Ogawa, K.; Zhang, Y.; Zhang, J.; Sangaroon, S.; Isobe, M.; Liu, Y. Predictive analysis for triton burnup ratio in HL-2A and HL-2M plasmas. *Plasma Physics and Controlled Fusion*. **2021**, *63*(4), 045013. https://doi.org/10.1088/1361-6587/abe054

[17] Dudson, B. (n.d.). *Welcome to FreeGS's documentation! — FreeGS 0.2.0 documentation*. Freegs.readthedocs.io. Retrieved September 25, 2023, from https://freegs.readthedocs.io/en/latest/

[18] The MathWorks, Inc. (n.d.). *Envelope Extraction - MATLAB & Simulink*. www.mathworks.com. Retrieved September 25, 2023, from https://www.mathworks.com/help/signal/ug/envelope-extraction-using-the-analytic-signal.html